4.4 Microstrip dipole

Basic theory

Microstrip antennas are frequently used in today's wireless communication systems. Thanks to their low profile, they can be mounted to the walls of buildings, to the fuselages of airplanes or to the reverse sides of mobile phones. Moreover, microstrip antennas are fabricated using the same technology as producing printed circuit boards. Therefore, the fabrication is relatively simple and well reproducible. Finally, microstrip antennas can be simply integrated directly to microwave circuits, which are based on microstrip technology, and therefore, no special transmission lines, symmetrization circuits or connectors are needed on the contrary to classical antennas [8].
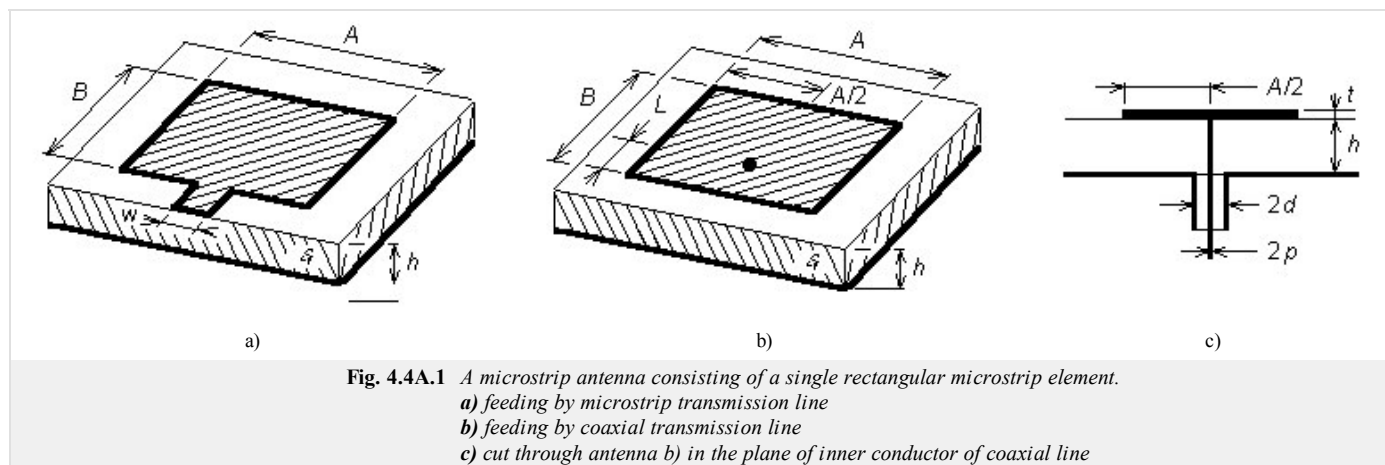
Nevertheless, there are several disadvantages of microstrip antennas. Narrow operation band is the main disadvantage. Due to this property, the design of microstrip antenna arrays exhibiting sufficiently low level of side-lobes is a really hard nut to be broken. Even the *parasitic radiation* of the feeding microstrip network, which can deform the directivity pattern [8].

One of the most frequently used types of microstrip antennas, the patch antenna, is depicted in fig. **4.4A.1a**. The antenna consists of a conductive rectangle of the dimensions $A \times B$, which is etched on a dielectric substrate. The antenna is fed by the microstrip transmission line (fig. **4.4A.1**, the microstrip goes from the front edge of the substrate crossways from the left). The second side of the substrate (on fig. **4.4A.1a** depicted as the bottom one) is continuously electroplated. The electroplated side plays the role of a *reflector* in the sense of zero potential (from the point of view of feeding) and in the sense of limiting radiation in the direction behind the reflector. Further, we call the electroplated side the ground plane.

The microstrip antenna that is fed by the microstrip transmission line (fig. **4.4A.1a**) can be considered as an open (non-shielded) open-ended transmission line, which is significantly widened at its end. If electromagnetic wave propagates along such transmission line, electromagnetic energy is primarily radiated into surrounding at the non-homogeneities (spontaneous widening of the microstrip at the border of the feeding line and the antenna element and the open end of this element) of the transmission line. The structure therefore behaves as a transmitting antenna. Moreover, if the length of the microstrip antenna element equals to the half of the wavelength on this widened transmission line, then input impedance of such an antenna is purely real [8]. Then, the antenna is said to be in resonance.

Radiation of a microstrip antenna can be explained in different ways. We can come out of the current distribution on the antenna element, which can be consequently understood as a wire antenna consisting of a very wide and a very thin antenna conductor. Next, we can come out from the line of electric intensity at the front side and at the back side of the antenna element (from the point of view of the feeding transmission line) and we can explain the radiation as an effect of a strong horizontal component (i.e. of the component, which is oriented in parallel with the ground plane) of electric field intensity vector at those edges.

As an alternative to the microstrip feeding of the microstrip antenna, a feeding by coaxial probe can be used (fig. **4.4A.1b**). Whereas the outer conductor of the coaxial cable is connected to the grounding plane, the inner conductor goes through a gap in the grounding plane and continues through the substrate to the microstrip antenna element, where it is fixed (fig. **4.4A.1c**). Significant reduction of the parasitic radiation of the feeding transmission line is the main advantage [8].

Fig. 4.4A.1 *A microstrip antenna consisting of a single rectangular microstrip element.*
a) feeding by microstrip transmission line
b) feeding by coaxial transmission line
c) cut through antenna b) in the plane of inner conductor of coaxial line

On the other hand, the coaxial feeding losses the main advantages of the microstrip feeding - a simple realization of a feeding system when microstrip antenna elements are grouped into arrays.

Now, turn our attention to the mathematical modeling of microstrip antennas.

Thanks to the popularity of microstrip antennas, several types of models of those antennas have been developed. Numerical models are of different validity domains (some are valid for *lower* microwave frequencies, some are valid for a limited interval of dimensions, etc.). Numerical models significantly differ even in their CPU-time demands (some models are based on closed-form expressions, which leads to low computational requirements, and some models are based on numerical methods, which leads to high CPU-time demands). The methods significantly differ even in the reached accuracy.

In the next, we concentrate on modeling microstrip antennas by the method of moments, which was described in the paragraph 4.1. As already said, the method comes out of Maxwell equations in the integral form, and therefore, we compute voltages and currents on the microstrip antenna element instead of searching for the distribution of electromagnetic field in the antenna surrounding.

In this paragraph, we are going to simplify the analysis. Instead of analyzing a patch antenna, we deal with a microstrip dipole (fig. **4.4A.2**) only. At the dipole, a small width of the antenna microstrip B is assumed. Then, only longitudinal currents (direction x) need to be considered and one-dimensional problem is going to be solved, which is an analogy to the solution of a wire dipole (paragraph 4.1)

Analyzing the antenna, we assume an infinitely wide substrate, infinitely small thickness of metallic layers $t \approx 0$, perfect electric conductivity of all metallic parts, lossless dielectrics and vacuum in the antenna surrounding.

Assume a plane wave of an angular frequency ω, which impinges the microstrip dipole. The electric field intensity vector $\mathbf{E}^I$ (the upper index I denotes the incident wave) describes the incident wave. This wave induces conductive currents in the antenna wire, which are described by the current density vector $\mathbf{J}$. Since the current has to be zero at the ends of the microstrip dipole, a charge described by the charge density ρ is accumulated here. In the following half-wave, the orientation of conductive currents is changed and the accumulated charge leaves the dipole [9].

a)   b)

Fig. 4.4A.2 *Microstrip dipole plus reflector.*
a) global view
b) discretization net for x component of current density

The effects of currents are described by the vector potential

$$\mathbf{A}(\mathbf{r}) = \iint_S \{G_A(\mathbf{r}|\mathbf{r}_0) \cdot \mathbf{J}(\mathbf{r}_0)\}dS_0 \qquad (4.4A.1a)$$

and the effects of charges are described by the scalar potential

$$V(\mathbf{r}) = \iint_S \{G_V(\mathbf{r}|\mathbf{r}_0)\rho(\mathbf{r}_0)\}dS_0. \qquad (4.4A.1b)$$

Value of the vector potential $\mathbf{A}(\mathbf{r})$ in the *observation pint* $\mathbf{r}$ on the microstrip dipole can be computed by the consecutive addition of contributions of components of the current density vector $\mathbf{J}$ from all the points of the microstrip antenna element $\mathbf{r}_0$ whereas the current density vector $\mathbf{J}$ is multiplied by the respective column of the dyadic Green function $\mathbf{G}_A$. The observation point, where the value of the vector potential is computed, is determined by the vector $\mathbf{r}$. Summation of contributions of all the currents flowing on the surface of the antenna element to the vector potential $\mathbf{A}(\mathbf{r})$ in the point $\mathbf{r}$ is performed by the integral over all the surface of the microstrip dipole S. The *source points*, where currents contributing to the vector potential to the point $\mathbf{r}$ are consecutively determined by the vector $\mathbf{r}_0$. The argument of the dyadic Green function $\mathbf{r}|\mathbf{r}_0$ shows the contribution of the current in $\mathbf{r}_0$ the potential in $\mathbf{r}$.

Dealing with the computation of the scalar potential, the dyadic Green function G_A is replaced by the scalar Green function G_V, and instead of the current density vector, the scalar charge density r appears. Except of this, eqn. (4.4A.1b) is identical with eqn. (4.4A.1a).

As already said, current density and charge density on the microstrip dipole are mutually associated. Therefore, eqns. (4.4A.1a) and (4.4A.1b) have to be completed by the continuity theorem given by

$$-j\omega\rho = \nabla \cdot \mathbf{J}. \qquad (4.4A.1c)$$

Eqn. (4.4A.1c) expresses the fact that current flowing from a closed region (see the current divergence as the right-hand side) has to equal to the charge reduction in this region within one second (see time derivative at the left-hand side).

If both the vector potential and the scalar one on the microstrip dipole are expressed, then the electric field intensity, which is radiated by the antenna, can be computed

$$\mathbf{E}^S = -j\omega\mathbf{A} - \nabla V. \qquad (4.4A.1d)$$

Time derivative of the vector potential $j\omega\mathbf{A}$ describes a *dynamic contribution* of electric charge on the dipole to the transmitted wave (electric conductive currents, i.e. charges in motion, are sources of vector potential). Gradient scalar potential gives a *static contribution* of electric charge on the dipole to the transmitted wave (static charges, which are concentrated this moment at the ends of the dipole, are sources of scalar potential).

The final problem, which has to be solved, are boundary conditions. Since all the metallic parts of the antenna are perfectly electrically conductive, components of electric field intensity, which are tangential to the antenna surface, have to be zero on this surface

$$\mathbf{n}_0 \times \mathbf{E}^S = -\mathbf{n}_0 \times \mathbf{E}^I. \qquad (4.4A.1e)$$

In the above-given relation, $\mathbf{E}^S$ denotes electric intensity of a wave, which is transmitted by the antenna, and $\mathbf{E}^I$ is electric intensity of a wave, arriving to the antenna from outside. The vector $\mathbf{n}_0$ is unitary vector, which is perpendicular to perfect electrically conductive surfaces.

As already explained in the paragraph 4.1, analytical solution of (4.4A.1) is unknown, and therefore, we utilize the moment method for its solution.

In the first step of the analysis of the microstrip dipole, the antenna is placed to Cartesian coordinate system (fig. **4.4A.2**). Next, vector equations (4.4A.1) are rewritten in the elected coordinate system to the scalar form. Moreover, we assume a special case when moving on the surface of the microstrip dipole (thanks to the boundary conditions, value of the tangential component of electric field intensity is known, which can be used further).

We start at eqn. (4.4A.1a), which describes dependency of vector potential on current density vector. The mutual relation between those two quantities is
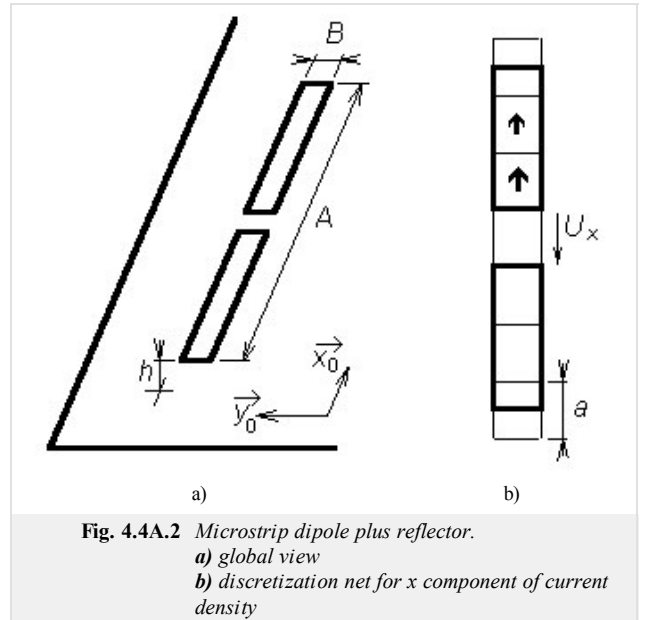
described by dyadic Green function. In a fact, dyadic Green function is a matrix 3×3 which elements are functions describing dependency of components x, y, z of vector potential on the components of current density vector. A single scalar element G_A^{st} of this dyadic Green function can be understood as s-th component of vector potential, which is *supplied* by an elementary electric dipole (described by a constant current density vector) in the direction t. Obviously, only the component xx of dyadic Green function is non-zero (assuming a very small width of the microstrip dipole, y-component of current density vector is zero and the only non-zero J_{xx} can be source of x-component of vector potential A_x; other components of vector **A** are of zero value).

If x component of vector potential (i.e., the component oriented along the dipole) is going to be computed, then (4.4A.1a) can be rewritten to

$$A_x(x_m, y_n) = \iint_S \left\{ G_A^{xx}(x_m, y_n | x', y') J_x(x', y') \right\} dx' dy'.$$

(4.4A.2)

Here, (x_m, y_n) are coordinates of a point on the surface of the dipole, where vector potential A_x is computed. Coordinates (x', y') specify the position of x-component of current density, which supplies x-component of vector potential. During the integration, coordinates (x', y') walk through all the points of the antenna surface S. The symbol J_x denotes x-component of current density vector, the symbol G_a^{xx} represents x diagonal term of dyadic Green function.

That way, (4.4A.1a) is adopted for the case of the analyzed antenna, and therefore, the attention is turned to the rearrangement of (4.4A.1b). Since (4.4A.1b) is a scalar equation containing scalar quantities only, the adoption consists in considering the introduced coordinated system

$$V(x_m, y_n) = \iint_S \left\{ G_V(x_m, y_n | x', y') \rho(x', y') \right\} dx' dy'.$$

(4.4A.3)

Again, scalar potential V is computed on the surface of the dipole in the point (x_m, y_n). Computing this potential, the product of scalar Green function G_V and charge density r is integrated over the whole surface of the dipole. The movement on the surface during integration is done by changing coordinates (x', y').

Next, we turn our attention to continuity equation (4.4A.1c). Since only x-component of current density vector is non-zero (conductive currents can flow in the direction of dipole axis only), the relation can be rewritten to the form

$$-j\omega\rho(x, y) = \frac{\partial J_x(x, y)}{\partial x}.$$

(4.4A.4)

Considering (4.4A.4), charge density r can be expressed as a function of current density J_x and can be substituted to (4.4A.3). That way, charge density is elliminated from (4.4A.3) and both potentials are expressed as functions of components of current density vector

$$V(x_m, y_n) - \frac{1}{j\omega} \iint_S \left\{ G_V(x_m, y_n | x', y') \left[\frac{\partial J_x(x', y')}{\partial x} \right] \right\} dx' dy'.$$

(4.4A.5)

Further, vector potential (4.4A.2) and scalar potential (4.4A.5) are substituted to (4.4A.1d), which enables us to compute electric field intensity of the radiated wave. Since both vector potential (4.4A.2) and scalar one (4.4A.5) are functions of an unknown current distribution on the surface of the dipole, even electric field intensity is a function of this current distribution

$$E_x^S(x_m, y_n) = -j\omega A_x(x_m, y_n) - \frac{\partial V(x_m, y_n)}{\partial x},$$

$$E_x^S(x_m, y_n) = -j\omega \iint_S \left\{ G_A^{xx}(x_m, y_n | x', y') J_x(x', y') \right\} dx' dy' + \frac{1}{j\omega} \iint_S \frac{\partial}{\partial x} \left\{ G_V(x_m, y_n | x', y') \left[\frac{\partial J_x(x', y')}{\partial x} \right] \right\} dx' dy'.$$

(4.4A.6)

Magnitude of electric field intensity on the surface of microstrip dipole can be determined, assuming perfect electric conductivity, from boundary condition (4.4A.1e). Current distribution J_x is the only unknown in (4.4A.6). And the equation (4.4A.6), which contains the unknown function $J_x(x, y)$, is going to be solved by moment method

The way of obtaining a piecewise-constant approximation of current distribution on the basis of (4.4A.6) was described in the paragraph 4.1. Therefore, the approach is here reminded only.

1. The region, where the solution of the integral equation is going to be found, has to be discretized (the surface of the dipole is divided to sub-regions, which do not overlap on one hand and which totally cover the whole analyzed dipole on the other hand (see fig. **4.4A.2b**).
   Performing discretization, boundary conditions have to be kept in mind. In our situation, x-component of current density J_x has to be zero at edges $x = 0$, $x = A$ because ends of the dipole can be understood as open ends of the microstrip transmission line.
   Exploiting piecewise constant approximation of current density components, boundary conditions can be met simply. The discretization mesh is extended behind the end of the dipole for one half of the discretization segment. Then, we enforce those extended segments to represent zero value of current (see fig. **4.4A.2b**).

2. The sought function $J_x(x, y)$ is approximated exploiting known basis functions (they are of unitary value over surface of a single discretization element and of zero value over the rest of elements) and unknown approximation coefficients

$$\tilde{J}_x^{(n)}(x, y) = \sum_{nx=1}^{Nx} J_x^{(nx)} \Pi^{(nx)}(x, y).$$

(4.4A.7)

   In the above-given relation, $\tilde{J}_x^{(n)}$ denotes approximation of x-component of current density over n-th discretization element, $J_x^{(nx)}$ is a *sample* of exact value of this component in the middle of n-th element, $\Pi^{(nx)}$ denotes basis function, which is unitary over the element nx and which is zero elsewhere, and Nx is total number of elements in the discretization mesh.

3. Approximation (4.4A.7) is substituted into the initial equation (4.4A.6). Since the approximation (4.4A.7) does not meet the initial equation (4.4A.6) exactly, we have to respect this fact adding the residual function $R_x(x, y)$ to (4.4A.6) together with the approximation (4.4A.7)

$$R_x(x, y) = E^S(x, y) - \sum_{nx=1}^{Nx} \left\{ J_x^{(nx)} \iint_S \left[G_A^{xx}(x, y | x', y') + \overline{G}_V(x, y | x', y') \right] dx' dy' \right\}.$$

(4.4A.8)

In these relations, G_A^{xx} is x diagonal term of dyadic Green function and using $\bar{G}_V$, partial derivative of scalar Green function is expressed.

Since basis functions Π are unitary over a respective element and are zero elsewhere, they do not have any representation in the above-given relations. Next, integration and summation were swapped, and the approximation coefficients J_x^{nx} were moved in front of the integral thank so their constant character.

4. Residual function $R_x(x, y)$ is going to be minimized. Lower values of the residual function are, closer our solution to the exact solution is. Minimization is done by the method of weighted residuals

$$\iint_S \{W_x(x, y)R_x(x, y)\}dxdy = 0. \tag{4.4A.9}$$

Here, R_x denotes the residual function computed according to (4.4A.8). The symbol W_x represents properly elected weighting functions. Weighting is done by Dirac pulses in order to eliminate one of integrations thanks to the filtering property

$$\iint_S \{\delta(x - x_m, y - y_n)R_x(x, y)\}dxdy = R_x(x_m, y_n). \tag{4.4A.10}$$

Accuracy of the method, which performs weighting by Dirac pulses, cannot be very good because the error is not minimized globally in the whole analyzed region but only in points, where Dirac pulses are of non-zero value (we operate with *moments* of residual function only).

5. Using the same number of weighting functions as the number of unknown approximation coefficients is, we obtain the set of N linear equations for N unknown coefficients. Solving this set of equations, we obtain unknown values of approximation coefficients, and therefore, approximation of the current distribution on the microstrip dipole can be composed. Considering known current distribution, the desired technical parameters of the antenna (input impedance, gain or directivity pattern) can be computed.

The whole algorithm described by the above points is given in detail in the layer B and in **[10]**, **[11]**. Replacing all the derivatives by central differences in the above-given algorithm, we obtain a matrix equation

$$\mathbf{U}_x = \mathbf{Z}_{xx}\,\mathbf{I}_x. \tag{4.4A.11}$$

In this equation, $\mathbf{U}_x$ is column vector of voltages in the direction x on discretization elements. This voltage is computed by multiplying x-component of electric field intensity by x-size of the discretization element

$$U_x(m, n) = E_x(m, n)a. \tag{4.4A.12}$$

The symbol a denotes the height of the discretization element (i.e. the size in the direction x).

Since the microstrip dipole is supposed to be fabricated from perfect electric conductor (voltage on this conductor is zero), the vector of voltages is filled in by zeros only except of elements relating to the excitation gap.

Next, $\mathbf{I}_x$ is column vector of currents in the direction x, which is unknown this moment for us. Elements of $\mathbf{I}_x$ are related to the component of current density J_x as follows

$$I_x(m, n) = J_x(m, n)B \tag{4.4A.13}$$

(B is the width of the dipole, and consequently the width of the discretization element). Impedance matrix $\mathbf{Z}_{xx}$ describes contribution of currents $\mathbf{I}_x$ and contribution of charge densities ρ (expressed from continuity equation (4.4A.4) using x-components of current density J_x on elements) to voltages $\mathbf{U}_x$ on those elements. Elements of the impedance matrix $\mathbf{Z}_{xx}$ are known (see the layer B)

$$Z_{xx}(m, n) = \frac{j\omega a}{B}\Gamma_A^{xx}(m, n) + \frac{1}{j\omega aB}\left[\Gamma_V(m^+, n^+) - \Gamma_V(m^-, n^+) - \Gamma_V(m^+, n^-) + \Gamma_V(m^-, n^-)\right]. \tag{4.4A.14}$$

In order to evaluate the impedance matrix $\mathbf{Z}_{xx}$, values of integrals of Green functions Γ_A^{xx} and Γ_V over the surface of the discretization element have to be computed for various distances between the source elements (over its surface, current distribution and charge one are integrated) and the observation one (on its surface, electric intensity is computed. Description of the numeric computation of those integrals in Matlab is given in the layer D.

Matlab program, which performs analysis of the microstrip dipole by the moment method, is described from user's point of view in the layer C. Here, we provide only illustration results obtained by the program.

For simplicity, the substrate between the dipole and the reflector is assumed to be of the same parameters as vacuum. If the dipole length equals to one half of wavelength and if the dipole width is $B = \lambda/1000$, following values of input impedance are obtained (in the first row of the table, the number of discretization elements to which antenna is subdivided is given):

Tab. 4.4A.1 *Input impedance for different number of discretization elements*

N	10	20	30	40
$R_{vst}\ [\Omega]$	95.2	97.3	98.0	98.4
$X_{vst}\ [\Omega]$	72.4	73.6	74.7	75.5

The results show the method to exhibit good stability with respect to the number of discretization elements. Moreover, the input impedance of the microstrip dipole with the reflector computed by moment method, is close to the results of analytical computations (sinusoidal current distribution J_x a wire dipole over an infinite planar reflector assumed). For a single wire dipole, radiation resistance of the antenna (related to the input) equals to $R_\Sigma = 85.6\ \Omega$.
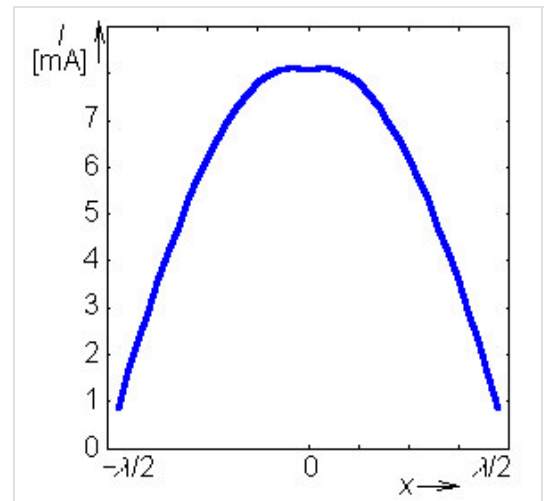
Investigating approximation of the distribution of *x*-component of the current along the microstrip dipole, we can show that depicting approximation coefficients from the vector **I_x** into a chart. That way, we obtain a course which is close to a sinusoidal current distribution (see fig. **4.4A.3**).

Fig. 4.4A.3 *Current distribution on half-wavelength symmetric microstrip dipole with planar reflector in the distance of one quarter of wavelength. Distribution computed for 40 cells.*